Stepwise amorphization of the flux-line lattice in $Ca_3Rh_4Sn_{13}$: A peak-effect study

S. Sarkar,* D. Pal, S. S. Banerjee, S. Ramakrishnan, and A. K. Grover†
Department of Condensed Matter Physics and Materials Science, Tata Institute of Fundamental Research, Colaba, Mumbai 400 005, India

C. V. Tomy
Department of Physics, Indian Institute of Technology, Powai, Mumbai 400 076, India

G. Ravikumar, P. K. Mishra, and V. C. Sahni
Technical Physics and Prototype Engineering Division, Bhabha Atomic Research Centre, Mumbai 400 085, India

G. Balakrishnan and D. McK. Paul
Department of Physics, University of Warwick, Coventry CV4 7AL, United Kingdom

S. Bhattacharya
Department of Condensed Matter Physics and Material Science, Tata Institute of Fundamental Research, Colaba, Mumbai 400 076, India
and NEC Research Institute, 4 Independence Way, Princeton, New Jersey 08540
(Received 20 September 1999; revised manuscript received 28 December 1999)

The peak effect (PE) region in a single crystal of $Ca_3Rh_4Sn_{13}$ is shown to comprise two discontinuous first-order-like transitions located near its onset and peak positions, in accordance with a stepwise fracturing of the flux-line lattice. Magnetization response to thermal cycling across the onset position produces an open hysteresis loop, consistent with the notion of the fracturing. A thermomagnetic history dependence study shows that the critical current density $J_c(H,T)$ is path dependent over a large part of the (H,T) parameter space. This path dependence ceases above the peak position of the peak effect, suggesting a complete amorphization of the flux-line lattice at (T_p,H_p) line. A plausible vortex phase diagram has been constructed for $Ca_3Rh_4Sn_{13}$ in which phases like an elastic solid, a plastic solid, and pinned and unpinned amorphous states have been identified.

I. INTRODUCTION

The peak effect (PE) phenomenon relates to an anomalous increase in the the critical current density (J_c) in a type-II superconductor before proceeding to zero at or close to the superconducting-normal phase boundary [$H_{c2}/T_c(H)$ line]. The PE is observed in a large variety of superconducting systems,[1–16] such as Nb,[7] V_3Si,[8] $2H$-$NbSe_2$,[1,10,11] $CeRu_2$,[2,5,6] $Yb_3Rh_4Sn_{13}$,[12,13] UPd_2Al_3 (heavy fermion superconductor),[3,4] $YBa_2Cu_3O_7$ (high-temperature superconductor),[15,16] etc. Two independent mechanisms have been widely considered to understand the PE phenomenon. A first one, originally due to Pippard,[17] attempts to relate the PE to a faster rate of decrease in the elastic moduli of the flux-line lattice (FLL) with an increase in the temperature as compared to that of the elementary pinning force. However, recently, Tachiki *et al.*[4] have suggested that the PE phenomenon in heavy fermion superconductors could be caused by the realization of a generalized Fulde-Ferrel-Larkin-Ovchinnikov[18,19] state that results in a first-order transition.

Modler *et al.*[3] have shown that the characteristics of the PE region in the heavy fermion compound UPd_2Al_3 are similar to those in the mixed valent compound $CeRu_2$ and the phase boundaries (locus of H and T) drawn for both of them extend over the similar parametric limits in the (H,T) space.[20] Sato *et al.*,[12] followed by Tomy *et al.*,[13] reported the observation of the PE and the construction of a magnetic phase diagram in the weakly pinned crystals of $Yb_3Rh_4Sn_{13}$, which bore striking resemblance to the similar phase diagrams in UPd_2Al_3 and $CeRu_2$.[3] Crabtree *et al.*[21] have shown the similarities in the transport properties in $CeRu_2$ and $YBa_2Cu_3O_7$ with those observed in the PE region of $2H$-$NbSe_2$.[1] The latter system, $2H$-$NbSe_2$, is thought to be an archetypal example for the classical scenario of the collapse of the elastic moduli of the FLL (implying a thermal and/or disorder induced amorphization of the FLL (Refs. 1 and 22) as a source of the PE. Very recently, Banerjee *et al.*[23] have shown that single crystals of $2H$-$NbSe_2$ and $CeRu_2$, having comparable levels of pinning, display fracturing of the vortex solid at or near the incipient FLL melting transition in both the systems.

Independent of these developments, Tomy *et al.*[24] have reported the occurrence of the PE and the construction of a magnetic phase diagram in $Ca_3Rh_4Sn_{13}$, which again bears striking resemblance to those in UPd_2Al_3 and $CeRu_2$.[3] This ternary system with a superconducting transition temperature of 8.18 K has the same crystal structure as that of $Yb_3Rh_4Sn_{13}$,[12,13] but, it does not contain any rare-earth ion. Low value (3.3×10^{-6} emu/cm^3) of the normal-state paramagnetic susceptibility precludes the realization of a Fulde-Ferrel-Larkin-Ovchinnikov state[4] in it. It is of interest to investigate in detail the PE region of $Ca_3Rh_4Sn_{13}$ and compare

the observed behavior with results in $2H$-$NbSe_2$ and $CeRu_2$.[23,25] Our studies reveal that the PE region in $Ca_3Rh_4Sn_{13}$ spans two sharp transitions located at its onset and peak positions and a characteristic hysteretic effect is observed on thermal cycling across the transition located at the onset. Prior to the peak position of the PE, the state of the vortex array and its current carrying capacity J_c depend on the thermomagnetic history, i.e., the J_c in the vortex array created in a field-cooled (FC) manner is much larger than that obtained in a zero-field-cooled (ZFC) manner.[25,26] The isothermal dc magnetization hysteresis experiments also reveal a characteristic path dependence in the J_c.

II. EXPERIMENTAL DETAILS

The single crystal of $Ca_3Rh_4Sn_{13}$ ($3.4\times3.2\times0.6$ mm^3, 48.1 mg) used in the present studies is grown by the tin flux method and it belongs to the same batch utilized by Tomy *et al.*[24] The ac susceptibility measurements in superposed dc magnetic fields have been performed using a well shielded home built ac susceptometer.[27] The ac and dc fields are coaxial and the sample is placed in such a way that one of its principal axes (cube edge) is always aligned parallel with the field (i.e., H//[001]). The ac measurements were made at a frequency of 211 Hz and with an ac amplitude of 1 Oe (rms). The dc magnetization data were obtained on a commercial superconducting quantum interference device (SQUID) magnetometer (Quantum Design Inc., U.S.A., Model MPMS 5), but using a different procedure designated as *half scan technique* by Ravikumar *et al.*[28] The magnetization values obtained via half scan technique minimize the artifacts arising due to the sample movement through the inhomogeneous magnetic field in a SQUID magnetometer and are independent of the choice of the scan length.

III. EXPERIMENTAL RESULTS

A. Manifestation of the peak effect via isofield ac susceptibility and isothermal dc magnetization measurements

1. Isofield ac susceptibility measurements

Figures 1(a) and (b) show the temperature dependence of the real part of the ac susceptibility [$\chi'(T)$] for $Ca_3Rh_4Sn_{13}$ in various dc bias fields. The FLL was prepared in the ZFC mode (i.e., the sample was initially cooled to the lowest temperature in zero magnetic field and subsequently a given value of the dc field was applied). The screening response was then measured while warming up the sample. The inset of Fig. 1(a) shows the typical variation of the $\chi'(T)$ in low applied fields (0 and 2.5 kOe). In zero field, the $\chi'(T)$ response shows perfect screening ($\chi'\approx-1$) at low temperatures and it undergoes a sharp transition towards the normal state near the superconducting transition temperature $T_c(0)$. As the applied field increases, the superconducting to normal transition broadens and the $\chi'(T)$ rises monotonically to its normal-state value at $T_c(H)$. However, for an applied dc field of 3.5 kOe, as shown in Fig. 1(a), this monotonic behavior is interrupted by the appearance of an anomalous dip in the $\chi'(T)$ at a temperature denoted as T_p(=7.43 K at 3.5 kOe).

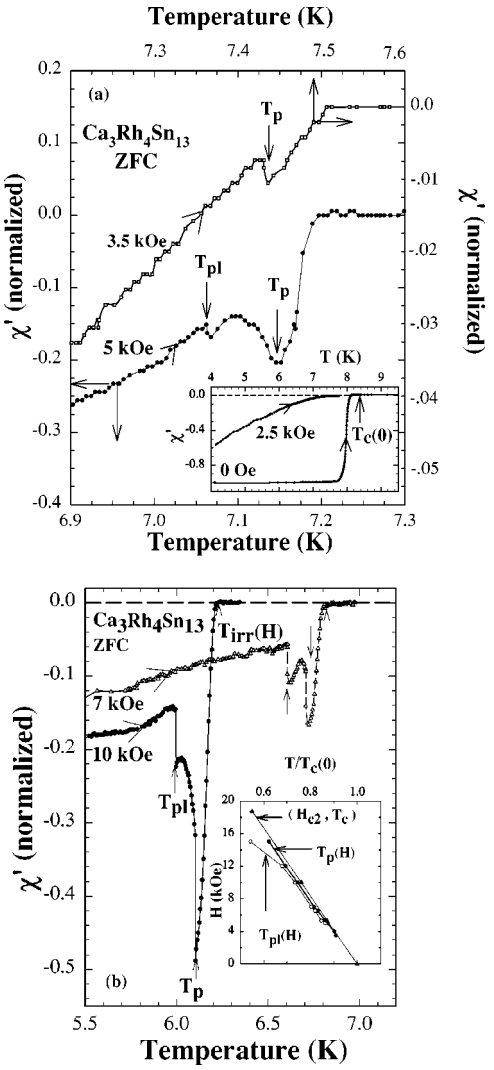

FIG. 1. (a) and (b) Temperature dependence of the real part of the ac susceptibility (χ') obtained for $Ca_3Rh_4Sn_{13}$. The inset in (a) shows typical behavior for low fields (0 Oe and 2.5 kOe). The curves in the main panel of (a) show the evolution of the structure in the PE as the dc field is increased. (b) shows the $\chi'(T)$ data for higher fields (7 and 10 kOe), where the double peak structure becomes prominent. The inset in (b) shows the T_{pl} and T_p lines, plotted in the thermomagnetic (H,T) phase space.

Within the Bean's critical state model,[29,15] the $\chi'(T)$ can be approximated as

$$\chi'(T)\sim-1+(\alpha h_{ac}/J_c), \tag{1}$$

where α is a geometrical factor, h_{ac} is the applied ac field and J_c is the critical current density. The above relation implies that the dip in the $\chi'(T)$ is a consequence of an enhancement in the J_c, the ubiquitous peak effect. As the dc bias field is increased further (from 3.5 to 5 kOe), the tiny dip in the $\chi'(T)$ transforms to a double peak structure [see Fig. 1(a)]. This two-dip structure becomes progressively more prominent as the dc field increases and the PE phenomenon eventually comprises two very sharp ($\leqslant$5 mK width) first-order-like transitions as implied by the data in Fig. 1(b). For instance, in a field of 10 kOe, the $\chi'(T)$ displays a sharp dip at $T=T_{pl}$ (defined as the onset temperature of the peak

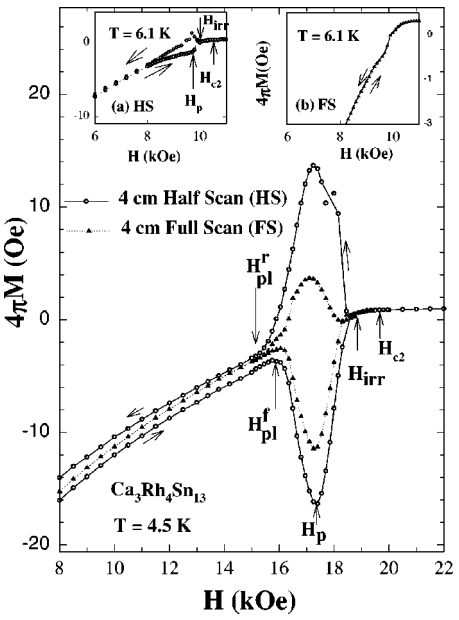

FIG. 2. The isothermal dc magnetization hysteresis data at 4.5 K with the full scan method and the half scan technique. H^f_{pl} and H^r_{pl} identify the fields at which the PE notionally commences on the forward leg and terminates on the reverse leg, respectively. The peak field, the irreversibility field, and the upper critical field are marked as H_p, H_{irr}, and H_{c2}, respectively. The two insets show the data at 6.1 K using the full scan method and the half scan technique.

effect), followed by another sharp dip at $T=T_p$ (the peak temperature). Above the T_p, the $\chi'(T)$ response shows a rapid recovery towards the zero value. These double peak features were not apparent in the isothermal $\chi'(H)$ scans performed by Tomy *et al.*[24] in the same crystal. However, the $T_p(H)$ values observed in the present isofield measurements show good agreement with the reported $H_p(T)$ values.[24]

The PE regime evolves rapidly with field and nearly a tenfold increase can be observed in the extent of the anomalous dip in the $\chi'(T)$ values characterizing the PE between $H_{dc}=3.5$ and 5 kOe. Also, the recovery of the $\chi'(T)$ above the T_p to its normal-state value becomes steeper as the field increases [cf. plots in Figs. 1(a) and (b)], thus indicating the sharpness of the transformation of vortex matter across the PE region. The inset of Fig. 1(b) summarizes the T_{pl} and T_p values, plotted in the (H,T) phase diagram, for various dc bias fields. Below 5 kOe, one can hardly distinguish between the T_{pl} and T_p values of the PE, and the T_{pl} and T_p curves appear to merge at a multicritical point corresponding to $T_p(H)/T_c(0)\sim 0.9$ in the phase diagram.

2. Isothermal dc magnetization results

In order to further explore the different facets of the PE observed in the ac susceptibility measurements, isothermal dc magnetization hysteresis measurements were also performed on the same crystal. The results at two temperatures are shown in Fig. 2. The magnetization curves were recorded for increasing as well as decreasing field cycles over a total scan length of 4 cm using the modified half scan technique as well as the conventional full scan method on a SQUID magnetometer. The magnetization data recorded at 4.5 K shows a clear hysteresis in the field interval of 15–19 kOe between the forward ($H\uparrow$) and the reverse ($H\downarrow$) legs of the field sweep. As per the Bean's critical state model,[29] this hysteresis in magnetization, $\Delta M(H)=M(H\uparrow)-M(H\downarrow)$, provides a measure of the macroscopic critical current density $J_c(H)$ and is a distinct indication of the occurrence of the PE in J_c. The field, where the magnetization hysteresis bubble is the widest, identifies the peak field H_p. The collapse of the hysteresis locates the irreversibility field H_{irr}, above which the critical current density falls below the measurable limit of the experimental method used (see Fig. 2).

From the main panel of Fig. 2, it is apparent that the hysteresis width in the peak effect region measured at 4.5 K by the half scan technique is significantly larger (and the hysteresis bubble is much more symmetric) than that measured using the conventional full scan procedure. It is also to be noted that the use of half scan technique results in measurable values of the magnetization hysteresis below the onset of the PE ($<H_{pl}$), whereas the full scan method results in the near absence of the magnetization hysteresis in the same field region (8–15 kOe in Fig. 2). The observed distinction is important in the sense that the isofield ac susceptibility measurements show a diamagnetic $\chi'(T)$ response [see Figs. 1(a) and (b)] prior to the arrival of the PE regime, which clearly demands that the dc magnetization should not be reversible (i.e., $J_c\neq 0$) prior to the PE. These results demonstrate the efficacy and the necessity of the half scan technique employed in our isothermal dc magnetization measurements. To illustrate the point even further, the two insets of Fig. 2 show a comparison of the magnetization hysteresis data obtained by half scan and full scan method at 6.1 K, where the peak field is expected to be about 10 kOe [cf. Fig. 1(b)].

Even while the peak effect hysteretic bubble recorded with the half scan technique at 4.5 K is more symmetric than that recorded with the full scan method, the difference in the fields marking the onset (H^f_{pl}) and the offset (H^r_{pl}) of the PE on the forward and reverse legs of the bubble persists, i.e., $H^f_{pl}>H^r_{pl}$. Hence this feature is not an artifact of the method used, but is a characteristic property of the system. Such difference in the onset and the offset fields of the PE has been widely noticed in several compounds like, UPd_2Al_3,[3] $CeRu_2$,[2] $2H$-$NbSe_2$,[23] $Yb_3Rh_4Sn_{13}$,[12,13] $YBa_2Cu_3O_7$,[30] etc., and have led to the proposition that the onset of the PE is akin to a first-order phase transition.[2,3,6,28,30] A first-order change allows for the possibility of the existence of the thermal hysteresis and the path dependence in the values of some physical variables, which in our case is the current density J_c.

B. Disorder and history dependence of the macroscopic critical current density J_c

1. Isofield ac susceptibility study

We now present the thermomagnetic history effects in the J_c in the PE region through the temperature-dependent ac susceptibility measurements. Two different sample histories, viz., the ZFC and the FCW, commonly associated with the disordered magnets such as spin glasses, were investigated. In the FCW mode, the sample was cooled down from the

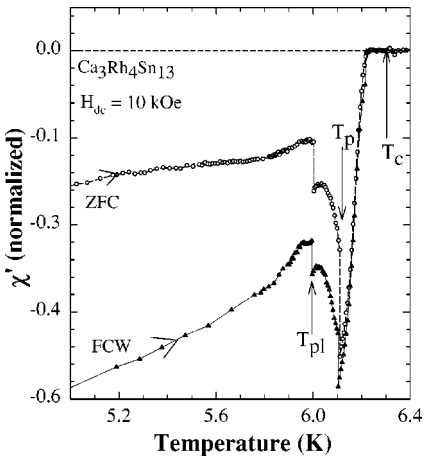

FIG. 3. The $\chi'(T)$ curves at $H=10$ kOe for two thermomagnetic histories, namely, zero-field-cooled (ZFC), and field-cooled (FCW) warmup. $\chi'(T)$ data show jumps at T_{pl} and T_p in both the plots, and just above T_p, the two curves merge into each other.

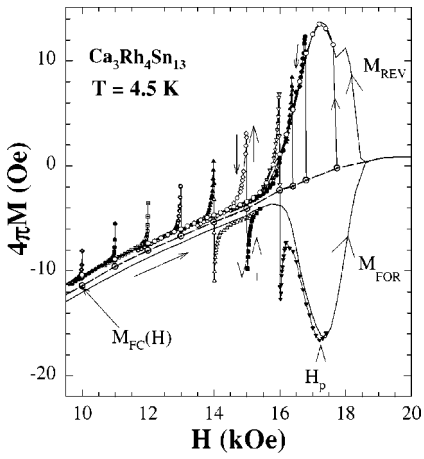

FIG. 4. Magnetization hysteresis (minor) loops obtained at 4.5 K after field cooling the sample in different preselected fields. The minor loops are obtained by either increasing or decreasing the field from a given $M_{FC}(H)$ value. Note that the envelope hysteresis loop is denoted by a continuous line.

normal state in the presence of the required dc field and then the measurements were performed while warming up the FLL. Figure 3 displays the typical response of the $\chi'(T)$ for the two thermomagnetic histories in a field of 10 kOe. The FLL states in the FCW mode can be seen to give larger diamagnetic screening response as compared to those produced via the ZFC mode over a wide range of temperature, but up to the peak position of the PE. Since the macroscopic current density J_c is directly related to the $\chi'(T)$ response [Eq. (1)], the differences in the $\chi'(T)$ responses between the ZFC and the FCW (field-cooled warmup) modes reveal the history dependence of the J_c in those modes, i.e., $J_c^{FCW}(T) > J_c^{ZFC}(T)$ for $T<T_p$. In an earlier report, Banerjee *et al.*[23] have exhibited the same kind of history dependence in $CeRu_2$ and $2H$-$NbSe_2$. Also, from the small-angle neutron-scattering study, Huxley *et al.*[31] have surmised that the FC state in $CeRu_2$ comprises more finely divided regions of correlated lattice as compared to those in the ZFC state. The difference in the ZFC and the FCW responses finally disappears at the peak position of the PE, somewhat akin to the magnetic responses in spin glasses where the ZFC and FC magnetization curves merge at the spin-glass transition temperature T_g.[32] However, unlike the spin glasses, where the glass temperature T_g could display measurable differences when the frequency and the amplitude of the ac field is varied, at least in the vortex system in $Ca_3Rh_4Sn_{13}$, both the onset (T_{pl}) and the peak (T_p) temperatures of the PE do not vary with the change in frequency and/or amplitude of the ac field.[37] The observed robust independence of T_{pl} and T_p on the amplitude and especially on the frequency, further attests the first-order nature of the transformations and the consequent absence of pretransitional fluctuation effects, such as critical slowing down, etc.

2. Isothermal dc magnetization data

To further illustrate the thermomagnetic history effects in the J_c, the magnetization hysteresis curves were recorded after obtaining the vortex states in the FC mode at fields lying well below as well as within the PE region, as shown in Fig. 4 at $T=4.5$ K. According to the Bean's critical state model,[33,34] when the critical current density is uniquely prescribed for a vortex state at a given H and T, the single-valued nature of the J_c demands that all the magnetization values obtained along the various paths with different thermomagnetic histories should lie within the envelope loop defined by the forward and the reverse branches of the magnetization curve. The dc magnetization data illustrated in Fig. 4 go beyond the above description and clarify the multivalued nature of the J_c. As the sample is field cooled in a preselected magnetic field ($H<H_p$) to the required temperature and the magnetization is recorded as a function of the increasing/decreasing fields, the initial magnetization values overshoot the forward/reverse magnetization envelope curves. On further increasing/decreasing the field, the magnetization values fall sharply and merge into the usual envelope loop (to be identified by the thin continuous line in Fig. 4). The overshooting of the initial magnetization values clearly indicates that the J_c value at a given field H in the FC state is higher than that in the ZFC state, in good agreement with the isofield ac susceptibility measurements discussed earlier. The observation that the FC magnetization curves eventually merge into the ZFC magnetization curve (i.e., the envelope loop) implies that the more strongly pinned FC vortex state heals to a more ordered ZFC state as the vortex state adjusts to a large enough change ΔH in the external dc field.[35] This change ΔH in the dc field required to anneal a given FC state to a neighboring ZFC state also increases as H approaches the peak field H_p, where the lattice is nearly amorphous[7] (ΔH varies from $\sim$2 kOe in the PE regime to $\sim$80 Oe well below the PE regime). The overshooting by the FC magnetization curve is, however, absent for fields greater than H_p (see Fig. 4). In such cases, the FC magnetization curve readily merges with the reverse envelope curve, since the history effect in the J_c disappears at the peak position of the PE, as seen earlier in the temperature dependent ac susceptibility data.

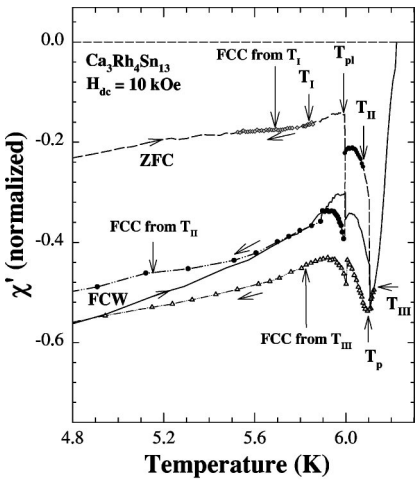

FIG. 5. $\chi'(T)$ responses obtained while thermal cycling across the onset (T_{pl}) and the peak (T_p) positions of the PE. T_I, T_{II}, and T_{III} identify the temperatures up to which the sample is warmed up each time after preparing the FLL in the ZFC mode.

C. Thermal/field cycling across the onset and the peak position of the peak effect: Evidence for shattering of the FLL

1. Thermal cycling during isofield ac susceptibility measurements

A deeper insight into the path dependence of the $\chi'(T)$ can be brought about by performing thermal cycling across the onset and the peak position of the PE as it yields striking evidence for the stepwise pulverization of the FLL.[23] The FLL prepared in the ZFC mode, after applying the required field, was warmed up to three preselected temperatures, T_I, T_{II}, and T_{III}, such that $T_I<T_{pl}$, $T_{pl}<T_{II}<T_p$, and $T_p<T_{III}<T_c$. The $\chi'(T)$ responses were then recorded while cooling down in the field from the above three preselected temperatures. The results are illustrated in Fig. 5, where the short-dashed and the solid lines (with data points omitted) are the responses produced in the ZFC and FC warmup modes, respectively (as shown earlier in Fig. 3). The cooling curves from the three preselected temperatures are represented by specific symbols. The following features are noteworthy in Fig. 5: (i) For cooling down the sample from a temperature below the onset of the peak effect ($T_I<T_{pl}$), the FC cooling curve retraces the ZFC warmup curve, which implies that, the changes in the FLL that occur along the ZFC path up to T_{pl} are reversible. (ii) When cooled down from a temperature T_{II}, the $\chi'(T)$ response initially tries to retrace the ZFC response, thereby effectively moving towards the ordered ZFC state. But close to T_{pl}, the $\chi'(T)$ response drops sharply to a value more diamagnetic than the ZFC curve (as well as more diamagnetic than the FC warmup response) thereby implying that the FLL gets far more disordered. This sharp jump towards a different, highly disordered state reveals a characteristic hysteretic behavior across the T_{pl} transition resulting in an open hysteresis loop, i.e., the $\chi'(T)$ response can never by itself (for $T<T_{pl}$) recover to the ZFC response. On cooling further down, the new $\chi'(T)$ curve cuts across the FC warm up response, thereby, becoming relatively less diamagnetic than the FC warmup curve down to the lowest temperatures. (iii) When the FLL is cooled down from a temperature above the peak position ($T_{III}>T_p$), the $\chi'(T)$ response initially retraces the FC warmup and the ZFC curves down to T_p. But below T_p, the $\chi'(T)$ response becomes more diamagnetic than both the ZFC and FC warmup responses. Between T_p and T_{pl}, this highly disordered state stages a partial recovery towards the FC warm up state, but it remains more disordered until merging with the FC warm up curve at low temperatures. These results bear close resemblance with the data in $2H$-$NbSe_2$ and $CeRu_2$,[23] and reaffirm the notion of the stepwise shattering process of the FLL across T_{pl} and T_p.

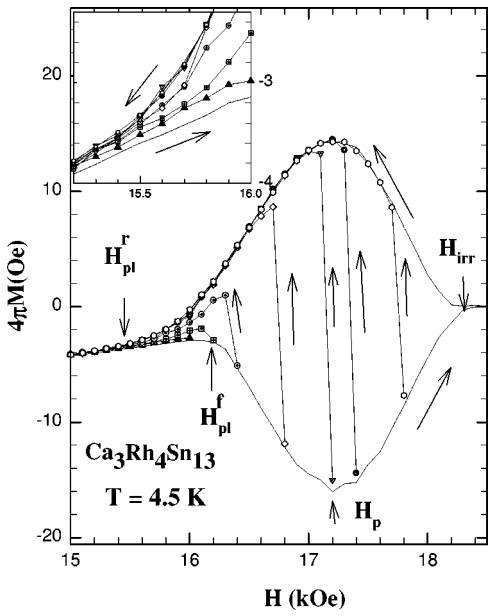

FIG. 6. Minor hysteresis loops generated by decreasing the field from the forward branch of the envelope loop at 4.5 K. The inset shows how the minor loops eventually merge into each other near H_{pl}^r on the reverse envelope loop.

2. Field cycling via minor hysteresis loops in the isothermal dc magnetization measurements

Another interesting manifestation of the path dependence of the J_c across the onset position of the PE can be seen in the isothermal dc magnetization hysteresis data via minor hysteresis loops, as reported by Roy and Chaddah[2] in several samples of $CeRu_2$ and its derivatives.[6,36] It was pointed out[2,6,30,36] that the minor hysteresis loops initiated from the fields lying in between the onset and the peak positions of the PE (i.e., for $H_{pl}<H<H_p$), saturate without merging with the reverse envelope loop. We show in Fig. 6 the behavior of the minor hysteresis curves initiated from the fields lying in between H_{pl}^f and H_p at 4.5 K in $Ca_3Rh_4Sn_{13}$. It is clear that the saturated (i.e., the highest) values of the minor loops do not meet the reverse envelope curve (identified by the continuous line). The inset of Fig. 6 shows how the minor loops eventually merge into the reverse envelope near H_{pl}^r. Note that the difference between the saturated value of a minor curve and the magnetization value on the reverse envelope curve decreases as the field from which the minor loop is initiated approaches the peak field H_p. For fields above H_p, the minor hysteresis curves readily merge into the reverse envelope curve since the J_c is path independent above H_p. An estimate of the current density values along the forward/reverse portion of the envelope loop between

TABLE I. Superconducting parameters in $Ca_3Rh_4Sn_{13}$ at $T=4.5$ K.

λ (Å)	κ	ξ (Å)	H_{c1} (Oe)	H_{c2} (Oe)	H_c (Oe)	G_i	j_0 (A/m^2)	$j_c(H=0)$ (A/m^2)
2270	17.5	130	110	19 500	800	3×10^{-7}	1.5×10^{11}	$\sim10^7$

H^f_{pl}/H^r_{pl} and H_p can be made by examining the respective half widths of the magnetization hysteresis loop.[35] The magnetization data of Fig. 6 leads to the inference that $J^f_c(H) < J^r_c(H)$. The inequality, $H^f_{pl} < H^r_{pl}$, and the distinct identities of the different minor loops vividly exemplify the irreversibility and the path dependence in the physical phenomenon that occurs across the onset position of the PE.

IV. DISCUSSION

A. Superconducting parameters of $Ca_3Rh_4Sn_{13}$

The superconducting parameters of the isotropic superconductor $Ca_3Rh_4Sn_{13}$ obtained from the ac susceptibility and dc magnetization data at 4.5 K using the Ginzburg-Landau theory[37] are given in Table I. The coherence length ξ and the penetration depth λ are $\sim$130 Å and $\sim$2270 Å, respectively, which correspond to a κ (λ/ξ) of 17.5. The presence of disorder, in the forms of thermal fluctuations (dynamic) and the quenched random pinning centers (static), governs the dynamics of the vortex array, and the two forms can be parametrized[38] by the value of the Ginzburg number [defined as $G_i=(1/2)(k_BT_c/H_c^2\xi^3\epsilon)^2$] and the ratio j_c/j_0 (where j_c and j_0 denote the depinning and depairing current densities, respectively). In order to conveniently observe the melting or the amorphization transition of the vortex lattice, the following two criteria must be fulfilled. First, the system must have an appreciably large value of the Ginzburg number, which guarantees an adequate separation of the vortex melting/amorphization curve from the H_{c2} line. Second, the system should have a sufficiently wide, weakly pinned region well below the superconductor-normal phase boundary, which could help to identify the occurrence of the PE in the magnetization experiments. The value of the Ginzburg number for $Ca_3Rh_4Sn_{13}$ is $\sim10^{-7}$, which is much smaller than the typical value ($\sim10^{-2}$) (Refs. 1 and 38) in high-T_c superconductors. It indicates that this compound has a rather narrow critical fluctuation region in the (H,T) phase space, where the vortex lattice can undergo melting transition due to the thermal fluctuations alone. However, the ratio j_c/j_0 is $\sim7\times10^{-5}$, which classifies $Ca_3Rh_4Sn_{13}$ among the weakly pinned systems. The weak pinning situation is very helpful as the structural and the dynamical behavior of the vortex array can be examined within the framework of the Larkin-Ovchinnikov collective pinning theory.[39,40] The small j_c/j_0 ratio in $Ca_3Rh_4Sn_{13}$ makes it an attractive candidate for the study of the pristine phase transitions of vortex matter.[38,41–43]

B. Collective pinning description

The motivation to invoke the Larkin-Ovchinnikov description[39] for explaining the observed behavior in $Ca_3Rh_4Sn_{13}$ is supported by the field dependence of the critical current density in it. The $J_c(H)$ can be estimated within the prescription of the critical state model[29] using the magnetization hysteresis data of Fig. 2 and the dimensions of the crystal.[33] Figure 7 shows the $J_c(H)$ vs H behavior at 4.5 K on a log-log plot. In the ZFC mode, J_c^{ZFC} displays a linear variation, which amounts to a power-law dependence for $J_c(H)$ prior to reaching the PE region at H_{pl}. Such a power-law dependence is often taken to be a signature of the collectively pinned elastic solid.[44] Figure 7 also includes the current density in the FC state estimated using the saturated values of the FC minor hysteresis curves initiated from different $M_{FC}(H)$ values (from Fig. 4). The difference between the highest magnetization value on the FC minor hysteresis curve initiated from a given H and the notional equilibrium magnetization value (defined as $[M_{FOR}+M_{REV}]/2$) could be taken as a measure of the $J_c^{FC}(H)$.[35] It is apparent from Fig. 7 that the difference between the J_c^{FC} and the J_c^{ZFC} values decreases as H decreases. For $H\leqslant4$ kOe, one cannot distinguish between the FC and the ZFC vortex states from the values of their critical current densities. A similar trend was noted[26] in $2H$-$NbSe_2$, where the difference between the J_c values in FC and the ZFC states ceased at about 1 kOe. In Larkin-Ovchinnikov model, the current density J_c is described by the pinning force equation:[39,40]

$$F_p=J_cH=(W/V_c)^{1/2}=[n_p\langle f_p^2\rangle/R_c^2L_c]^{1/2}, \qquad (2)$$

where W and V_c represent the pinning parameter and the correlation volume of a Larkin domain within which the FLL is undistorted and well correlated, despite the presence of pinning, respectively. n_p is the density of the pinning centers (pins), f_p is the elementary pinning interaction proportional to the condensation energy, and R_c and L_c are the radial and longitudinal correlation lengths. The pinning interaction is expected to decrease with increasing temperature, which corresponds to a monotonic decrease in the J_c. Thus the anomalous increase in the J_c across the PE region can be rationalized only by an introduction of an anomalous sudden drop in the Larkin volume V_c. The two discontinuous jumps in J_c in

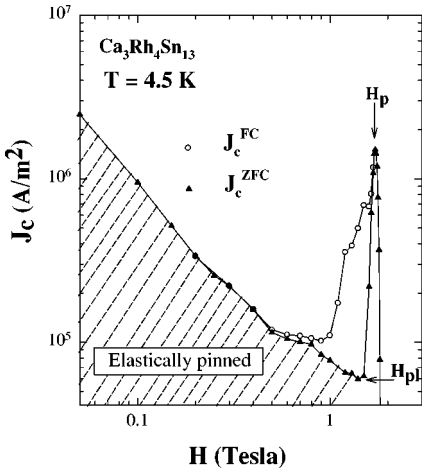

FIG. 7. Log-log plot of J_c vs H in the ZFC and FC modes at $T=4.5$ K.

the $\chi'(T)$ data therefore imply sudden shrinkages of the V_c at T_{pl} and T_p. This picture proposes that for a sample with substantial pinning, the competition between the interaction and the disorder leads to some threshold behaviors. When the pinning energy overcomes the elastic energy of the FLL, which is continuously softened due to increase in the temperature, a disorder induced transition transforms the FLL from an elastic medium to a plastically deformed vortex states with a proliferation of the topological defects (dislocations) at the onset of the PE (corresponding to the first jump at T_{pl}).[23] At a higher temperature, the thermal energy overcomes the elastic energy and produces a complete amorphization of the vortex solid at the peak position of the PE [where the second jump in $\chi'(T)$ is located].

The crucial support for the stepwise fracturing of the FLL comes from the thermal cycling experiments performed on a well-ordered FLL (see Fig. 5). While cooling down from a temperature within the PE pocket (from T_{II} in Fig. 5), the FLL is cooled from a partially fractured, plastically deformed state. So the FLL initially tries to heal towards the well ordered ZFC state. But, as the temperature decreases progressively towards T_{pl}, the decrease in the strength of the thermal fluctuations start to stiffen the FLL, thereby building up the stresses. The system thus fails to drive out the dislocations in order to heal back to the ZFC state. Instead, it shatters further to release the stresses and reaches a different metastable state. To reach back to the ZFC state from this metastable state, one needs to shake the FLL vigorously by an external driving force.[35] This characteristic hysteretic behavior across the T_{pl} transition is definitely novel; it is not usually seen across a typical first-order (melting) transition in the absence of disorder.

The difference between the vortex states formed during the cooldown from $T>T_p$ (from T_{III} in Fig. 5) and the one which evolves during the FC warm up mode probably originates from the slow dynamics[1,23,26] of the order-disorder transformation across the T_{pl} and the T_p. We believe that above T_p, the FLL transforms into a completely pulverized state, which is so disordered that the FLL correlations beyond the first few nearest-neighbor intervortex spacings are immaterial. Thus, if the FLL is cooled down from such a disordered state ($T>T_p$), one cools in the liquidlike correlations and the FLL remains in an amorphous state (supercooled state) down to a much lower temperature (than that during the FC warmup cycle). The above scenario leads us to conclude that at T_{pl}, the FLL transforms from a nearly defect-free ordered lattice, such as a Bragg glass phase,[41,42] to a highly defective plastically deformed lattice[41–43,46–49] with full of topological defects analogous to a vortex glass phase. Then at T_p, the vortex glass phase further transforms into a completely amorphous but pinned phase ($J_c\neq 0$), above which the lattice is no longer correlated and loses its history and memory. The vanishing of the pinning occurs at an even higher temperature marked as the irreversibility temperature T_{irr}.

The path dependence in the $\chi'(T)$ response for $T\ll T_p$ is a thought provoking result. It has been shown[50] that the magnetization in the ZFC state (M_{ZFC}) differs from magnetization in the FC state (M_{FC}) up to T_{irr}, and hence one could produce a hierarchy of states whose bulk magnetization values lie in between the ZFC and the FC states. In the ZFC state, one typically establishes a critical state with the critical current density $J_c(H)$. The states with magnetization lying in between M_{ZFC} and M_{FC} would be in subcritical state with current densities $J(H)\leqslant J_c(H)$.[51] At T_{irr}, the $J_c(H)$ approaches the depinning limit ($J_c\rightarrow 0$). The magnetic shielding responses, as measured via the $\chi'(H,T)$ values, of all the states whose magnetization values lie in between M_{ZFC} and M_{FC} are dictated by the same $J_c(H)$, i.e., the $\chi'(T)$ values do not display any path dependence though the magnetization values are path dependent. On the contrary, we witness a thermomagnetic history dependence in $J_c(H)$ for the FLL states prepared via different paths in $Ca_3Rh_4Sn_{13}$. The quenched random disorder appears to pin the vortices into different configurations while preparing the vortex states via different routes in the (H,T) plane and this leads to its history dependence. The ZFC state with smallest $\chi'(T)$ response is perhaps the most ordered state with the lowest J_c and the slowly cooled FC state is the most disordered state with the largest J_c. Thus one can produce a hierarchy of metastable states whose J_c values lie in between the J_c^{ZFC} and the J_c^{FC}. The history dependence of the $\chi'(T)$ response disappears at the peak position (T_p) of the PE, presumably due to the fact that the FLL prepared in any manner almost completely amorphizes at the peak position and the vortex system loses order in equilibrium.

C. Determination of R_c and L_c by the collective pinning analysis

Within the LO framework of collective pinning, the dimensionality (D) of the collective pinning is determined by the relative magnitude of longitudinal correlation length L_c of a Larkin domain with respect to the thickness d of the sample.[38–40] Thus a transition from three-dimensional (3D) to 2D behavior is predicted, when $L_c\geqslant d/2$. The estimated value of $L_c(0)$ $\{L_c(0)=\xi(0)[j_0(T)/j_c(0)]^{1/2}\}$ from the j_0/j_c ratio for $Ca_3Rh_4Sn_{13}$ is 1.6 μm, which is much smaller than $d/2$ of the present crystal. We have therefore estimated the field dependence of the longitudinal and transverse correlation lengths, $L_c(H)$ and $R_c(H)$ within the framework of 3D collective pinning, at 4.5 K using various superconducting parameters calculated from isotropic GL theory (cf. Table I).

The longitudinal and the transverse correlation lengths are connected by the equation (A. Angurel *et al.*[40])

$$L_c=(c_{44}/c_{66})^{1/2}R_c\approx(2\sqrt{2}/\pi\xi)(b/1-b)^{1/2}R_c^2, \qquad (3)$$

where c_{66} and c_{44} are the shear and the tilt moduli, respectively, ξ is the coherence length, and b is the reduced field parameter H/H_{c2}. Substituting the expressions for c_{66} and c_{44} (Ref. 40) in the above equation and incorporating it with the LO equation for collective pinning [Eq. (2)], one can determine R_c and L_c as

$$R_c=[W_0b(1-b)^2]/\{2\sqrt{2}/\pi\xi[b/(1-b)]^{1/2}\}^{1/4}(1/J_cH)^{1/2}, \qquad (4)$$

$$L_c=\{2\sqrt{2}/\pi\xi[b/(1-b)]^{1/2}\}^{1/2}[W_0b(1-b)^{1/2}]^{1/2}(1/J_cH). \qquad (5)$$

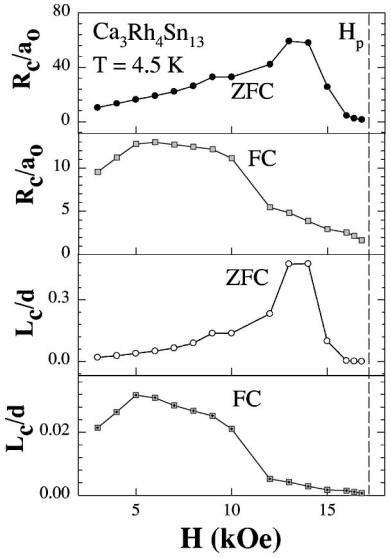

FIG. 8. Plot of the computed values of the ratios R_c/a_0 and L_c/d versus field at $T=4.5$ K for $Ca_3Rh_4Sn_{13}$.

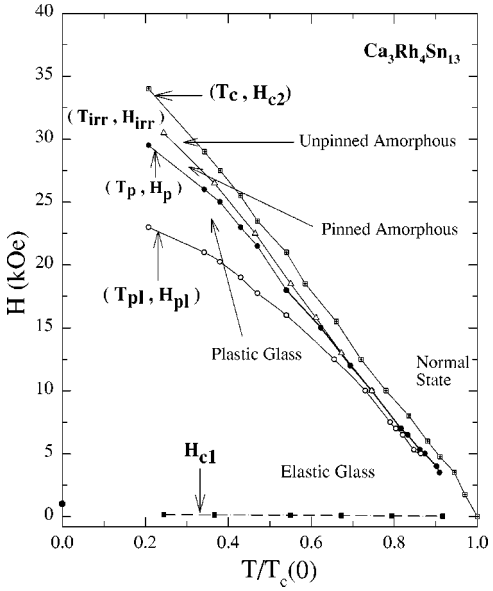

FIG. 9. Vortex phase diagram for $Ca_3Rh_4Sn_{13}$ depicting H_{c1}, (H_{pl},T_{pl}), (H_p,T_p), (H_{irr},T_{irr}), and (H_{c2},T_c) lines. For nomenclature, see text.

Figure 8 summarizes the computed data for the field dependence of the ratios R_c/a_0 and L_c/d for the FLL at 4.5 K in both the ZFC and the FC modes. For the ZFC mode, both R_c/a_0 and L_c/d initially increase with the field up to the onset field H_{pl} of the PE. But, between H_{pl} and H_p, they decline rapidly, which indicates that the elastic energy decays much faster than the pinning energy as the R_c and the L_c decay faster than the pinning parameter W. Near the peak field H_p, the ratio $R_c/a_0 \rightarrow 1$, which supports the view that the FLL gets completely amorphized as the shear modulus c_{66} collapses. However, for the FC state, both the R_c/a_0 and the L_c/d show weaker dependence up to $0.8H_{pl}$, after which they start to decrease gradually, reaching the amorphous limit near H_p.

D. Vortex phase diagram

Collating all the ac susceptibility and dc magnetization data (including those from Ref. 24), we can finally construct a vortex phase diagram for $Ca_3Rh_4Sn_{13}$ as shown in Fig. 9. The lower critical field line $H_{c1}(T)$ has been obtained from an analysis of the isothermal dc magnetization measurements performed at low fields.[37] The H_{c2} line has been derived from the values obtained from the ac susceptibility as well as the dc magnetization data. The regime in the magnetic phase diagram enclosed by these two lines identifies the mixed state of a type-II superconductor. After the discovery of high-T_c superconductors an extra line, designated as an irreversibility line, has been introduced[50] in the phase diagram of type-II superconductors, which marks the predominance of the influence of thermal fluctuations on the vortices. In weakly pinned systems, the competition and interplay between the static (quenched random pinning) and dynamic (thermal fluctuations) disorder and the elasticity of the lattice create a richer phase diagram comprising a few more lines within the mixed phase. These lines reflect how the nearly defect-free (very small j_c/j_0 ratio) elastically deformed vortex lattice gets disordered in steps. The onset of the PE, which is identified with the $T_{pl}(H)$ in ac susceptibility data and the $H_{pl}(T)$ in the dc magnetization data is drawn as (H_{pl},T_{pl}) line in Fig. 9. This line marks the onset of shattering of the FLL as the pinning energy overcomes the elastic energy resulting in a transition from an elastic solid similar to a Bragg glass phase to a plastically deformed vortex state. The shattering of the FLL gets completed at the peak position of the PE [marked as (H_p,T_p) line in Fig. 9] producing a near collapse of the Larkin domain and the complete amorphization of the FLL, thereby representing a transformation to a highly viscous pinned amorphous state.

If we choose to identify (H_p,T_p) line in Fig. 9 with the FLL melting curve $(B_m,\ T)$, given by the relation[38]

$$B_m=\beta_m(c_L^4/G_i)H_{c2}(0)(T_c/T)^2 \times\{1-(T/T_c)-[B_m/H_{c2}(0)]\}^2, \quad (6)$$

then the Lindemann number c_L is found to be ~ 0.1, which is reasonable in the context of similar estimates for $CeRu_2$ and $NbSe_2$.[23] In Eq. (6), we used G_i and $H_{c2}(0)$ as 1.3×10^{-7} and 4.5 T, respectively, and β_m was taken as 5.6 from Ref. 38. For higher fields (i.e., above H_{irr} line), the critical current density vanishes as identified by the vanishing of the hysteresis in the dc magnetization data. The irreversibility line marks a crossover (presumably dynamic) from a pinned amorphous to an unpinned amorphous state.

V. CONCLUSION

In summary, the peak effect, an anomalous upturn in the critical current density of superconductors, has been investigated in detail for the superconducting system $Ca_3Rh_4Sn_{13}$ via isofield ac and isothermal dc magnetization measurements. A structure in the peak effect region, comprising two first-order-like jumps at the onset (T_{pl}) and the peak (T_p) positions of the PE, has been observed in the isofield ac susceptibility measurements. Our ansatz about this two-peak structure is that the first peak reflects the commencement of a

pinning induced stepwise shattering of the FLL through the sudden shrinkage of the correlation (Larkin) volume V_c at T_{pl}.[23,45] The thermal cycling across the T_{pl} reveals an open hysteresis loop across it, which is a spectacular manifestation of the shattering phenomenon of the FLL. The macroscopic current density J_c of $Ca_3Rh_4Sn_{13}$ shows pronounced thermomagnetic history dependence below T_p, which reveals the role played by quenched random disorder on the FLL. The disappearance of history dependence above T_p reflects the absence of memory of any previous history and the complete amorphization of the FLL. The two-peak structure becomes inconspicuous below a certain dc field indicating a possible crossover from an interaction dominated regime to a pinning dominated regime when the lattice constant a_0 becomes comparable to the penetration depth, which measures the range of the electromagnetic interaction between the vortices. Finally, the vortex phase diagram of $Ca_3Rh_4Sn_{13}$ is constructed which shows close resemblance to phase diagrams drawn earlier for $CeRu_2$ and $2H$-$NbSe_2$.[23] This could further lead to the establishment of a generic phase diagram for all conventional low-T_c type-II superconductors in the presence of quenched random disorder and thermal fluctuations.

ACKNOWLEDGMENT

The work at University of Warwick was supported by a research grant from EPSRC, U.K.

*Electronic address: shampa@tifr.res.in

†Electronic address: grover@tifr.res.in

[1] S. Bhattacharya and M. J. Higgins, Phys. Rev. Lett. **70**, 2617 (1993); M. J. Higgins and S. Bhattacharya, Physica C **257**, 232 (1996), and references therein.

[2] A. D. Huxley, C. Paulsen, O. Laborde, J. L. Tholence, D. Sanchez, A. Junod, and R. Calemczuk, J. Phys.: Condens. Matter **5**, 7709 (1993); S. B. Roy and P. Chaddah, *ibid.* **9**, L625 (1997).

[3] R. Modler, P. Gegenwart, M. Lang, M. Deppe, M. Weiden, T. Luhmann, C. Geibel, F. Steglich, C. Paulsen, J. L. Tholence, N. Sato, T. Komatsubara, Y. Onuki, M. Tachiki, and S. Takahashi, Phys. Rev. Lett. **76**, 1292 (1996).

[4] M. Tachiki, S. Takahashi, P. Gegenwart, M. Weiden, M. Lang, C. Geibel, F. Steglich, R. Modler, C. Paulsen, and Y. Onuki, Z. Phys. B: Condens. Matter **100**, 369 (1996).

[5] N. R. Dilley, J. Herrmann, S. H. Han, M. B. Maple, S. Spagne, J. Diederichs, and R. E. Sager, Physica C **265**, 150 (1996).

[6] S. B. Roy, Philos. Mag. B **65**, 1453 (1992); K. Yagasaki, M. Hedo, and T. Nakama, J. Phys. Soc. Jpn. **62**, 3825 (1993); S. B. Roy, P. Chaddah, and S. Chaudhary, J. Phys.: Condens. Matter **10**, 4885 (1998).

[7] P. L. Gammel, U. Yaron, A. P. Ramirez, D. J. Bishop, A. M. Chang, R. Ruel, L. N. Pfeiffer, E. Bucher, G. D'Anna, D. A. Huse, K. Mortensen, M. R. Eskildsen, and P. Kes, Phys. Rev. Lett. **80**, 833 (1998).

[8] M. Isino, T. Kobayashi, N. Toyota, T. Fukase, and Y. Muto, Phys. Rev. B **38**, 4457 (1988).

[9] J. G. Park, M. Ellerby, K. A. McEwen, and M. de Podesta, J. Magn. Magn. Mater. **140-144**, 2057 (1995).

[10] U. Yaron, P. L. Gammel, D. A. Huse, R. N. Kleiman, C. S. Oglesby, E. Bucher, B. Batlogg, D. J. Bishop, K. Mortensen, K. Clausen, C. A. Bolle, and F. de la Cruz, Phys. Rev. Lett. **73**, 2748 (1994).

[11] C. A. Bolle, F. de la Cruz, P. L. Gammel, J. V. Waszczak, and D. J. Bishop, Phys. Rev. Lett. **71**, 4039 (1993); F. Pardo, F. de la Cruz, P. L. Gammel, C. S. Oglesby, E. Bucher, B. Batlogg, and D. J. Bishop, *ibid.* **78**, 4633 (1997).

[12] H. Sato, Y. Akoi, H. Sugawara, and T. Fukahara, J. Phys. Soc. Jpn. **64**, 3175 (1995).

[13] C. V. Tomy, G. Balakrishnan, and D. Mck. Paul, Physica C **280**, 1 (1997).

[14] K. Hirata, H. Takeya, T. Mochiku, and K. Kadowaki, in *Advances in Sperconductivity VIII*, edited by H. Hayakawa and Y. Enomoto (Springer-Verlag, Tokyo, Japan, 1996), p. 619.

[15] X. Ling and J. I. Budnick, in *Magnetic Susceptibility of Superconductors and Other Spin Systems*, edited by R. A. Hein, T. L. Francavilla, and D. H. Liebenberg (Plenum Press, New York, 1991), p. 377.

[16] G. D'Anna, W. Benoit, W. Sadowski, and E. Walker, Europhys. Lett. **20**, 167 (1992); H. Küpfer, Th. Wolf, C. Lessing, A. A. Zhukov, X. Lancon, R. Meier-Hirmer, W. Schauer, and H. Wühl, Phys. Rev. B **58**, 2886 (1998), and references therein.

[17] A. B. Pippard, Philos. Mag. **19**, 217 (1969); A. M. Campbell and J. E. Evetts, Adv. Phys. **21**, 327 (1972), and references therein.

[18] P. Fulde and R. A. Farrell, Phys. Rev. **135A**, 550 (1964).

[19] A. I. Larkin and Y. N. Ovchinnikov, Zh. Éksp. Teor. Fiz. **47**, 1136 (1964) [Sov. Phys. JETP **20**, 762 (1965)].

[20] K. Gloos, R. Modler, H. Schimanski, C. D. Bredl, C. Geibel, F. Steglich, A. I. Buzdin, N. Sato, and T. Komatsubara, Phys. Rev. Lett. **70**, 501 (1993); A. Ishiguro, A. Sawada, Y. Inada, J. Kimura, M. Suzuki, N. Sato, and T. Komatsubara, J. Phys. Soc. Jpn. **64**, 378 (1995).

[21] G. W. Crabtree, M. B. Maple, W. K. Kwok, J. Herrmann, J. A. Fendrich, N. R. Dilley, and S. H. Han, Phys. Essays **9**, 628 (1996).

[22] C. Tang, X. S. Ling, S. Bhattacharya, and P. M. Chaikin, Europhys. Lett. **35**, 597 (1996), and references therein.

[23] S. S. Banerjee, N. G. Patil, S. Saha, S. Ramakrishnan, A. K. Grover, S. Bhattacharya, G. Ravikumar, P. K. Mishra, T. V. C. Rao, V. C. Sahni, M. J. Higgins, E. Yamamoto, Y. Haga, M. Hedo, Y. Inada, and Y. Onuki, Phys. Rev. B **58**, 995 (1998).

[24] C. V. Tomy, G. Balakrishnan, and D. McK. Paul, Phys. Rev. B **56**, 8346 (1997).

[25] G. Ravikumar, V. C. Sahni, P. K. Mishra, T. V. C. Rao, S. S. Banerjee, A. K. Grover, S. Ramakrishnan, S. Bhattacharya, M. J. Higgins, E. Yamamoto, Y. Haga, M. Hedo, Y. Inada, and Y. Onuki, Phys. Rev. B **57**, R11 069 (1998).

[26] W. Henderson, E. Y. Anderi, M. J. Higgins, and S. Bhattacharya, Phys. Rev. Lett. **77**, 2077 (1996); **80**, 381 (1998).

[27] S. Ramakrishnan, S. Sundaram, R. S. Pandit, and G. Chandra, J. Phys. E **18**, 650 (1985).

[28] G. Ravikumar, T. V. C. Rao, P. K. Mishra, V. C. Sahni, S. S. Banerjee, A. K. Grover, S. Ramakrishnan, S. Bhattacharya, M. J. Higgins, E. Yamamoto, Y. Haga, M. Hedo, Y. Inada, and Y. Onuki, Physica C **276**, 9 (1997); **298**, 122 (1998).

[29] C. P. Bean, Rev. Mod. Phys. **36**, 31 (1964).

[30] S. Kokkaliaris, D. A. J. de Groot, S. N. Gordeev, A. A. Zhukov, R. Gagnon, and L. Taillefer, Phys. Rev. Lett. **82**, 5116 (1999).

[31] A. Huxley, R. Cubitt, D. McK. Paul, E. Forgan, M. Nutley, H.

Mook, M. Yethiraj, P. Lejay, D. Caplan, and J. M. Penisson, Physica B **223&224**, 169 (1996).
[32] J. A. Mydosh, *Spin Glasses: An Experimental Introduction* (Taylor and Francis, London, 1993).
[33] P. Chaddah, in *Studies in High Temperature Superconductors*, edited by A. V. Narlikar (Nova Science Inc., Commack, NY, 1995), Vol. 14, pp. 245-274.
[34] A. K. Grover, in *Studies in High Temperature Superconductors* (Ref. 33), Vol. 14, pp. 185-244.
[35] S. S. Banerjee, N. G. Patil, S. Ramakrishnan, A. K. Grover, S. Bhattacharya, G. Ravikumar, P. K. Mishra, T. V. C. Rao, V. C. Sahni, and M. J. Higgins, Appl. Phys. Lett. **74**, 126 (1999).
[36] S. B. Roy, P. Chaddah, S. Chaudhary, and L. F. Cohen, *Proceedings of the 41st Annual DAE Solid State Physics Symposium* (Universities Press, Hyderabad, India, 1998), Vol. 41, p. 367.
[37] S. Sarkar *et al.* (unpublished).
[38] G. Blatter, M. V. Feigel'man, V. B. Geshkenbein, A. I. Larkin, and V. M. Vinokur, Rev. Mod. Phys. **66**, 1125 (1994).
[39] A. I. Larkin and Y. N. Ovchinnikov, Zh. Éksp. Teor. Fiz. **65**, 1704 (1973) [Sov. Phys. JETP **38**, 854 (1974)]; A. I. Larkin, J. Low Temp. Phys. **34**, 409 (1979).
[40] R. Wordenweber, P. H. Kes, and C. C. Tsuei, Phys. Rev. B **33**, 3172 (1986); L. A. Angurel, F. Amin, M. Polichetti, J. Aarts, and P. H. Kes, *ibid.* **56**, 3425 (1997).
[41] T. Giamarchi and P. Le. Doussal, Phys. Rev. Lett. **72**, 1530 (1994).
[42] T. Giamarchi and P. Le. Doussal, Phys. Rev. B **52**, 1242 (1995).
[43] M. Gingras and D. A. Huse, Phys. Rev. B **53**, 15 193 (1996).
[44] A. Durate, E. F. Righi, C. A. Bolle, F. de la Cruz, P. L. Gammel, C. S. Oglesby, E. Bucher, B. Batlogg, and D. J. Bishop, Phys. Rev. B **53**, 11 336 (1996).
[45] S. S. Banerjee, N. G. Patil, S. Ramakrishnan, A. K. Grover, S. Bhattacharya, G. Ravikumar, P. K. Mishra, T. V. C. Rao, V. C. Sahni, M. J. Higgins, C. V. Tomy, G. Balakrishnan, and D. McK. Paul, Phys. Rev. B **59**, 6043 (1999).
[46] S. Bhattacharya and M. J. Higgins, Phys. Rev. B **49**, 10 005 (1994).
[47] S. Bhattacharya and M. J. Higgins, Phys. Rev. B **52**, 64 (1995).
[48] S. Ryu, M. Hellerquist, S. Doniach, A. Kapitulnik, and D. Stroud, Phys. Rev. Lett. **77**, 5114 (1997).
[49] M. C. Faleski, M. C. Marchetti, and A. A. Middleton, Phys. Rev. B **54**, 12 427 (1996).
[50] K. A. Müller, M. Takashige, and J. G. Bednorz, Phys. Rev. Lett. **58**, 1143 (1987).
[51] P. Chaddah and G. Ravikumar, Pramana **31**, L141 (1988).